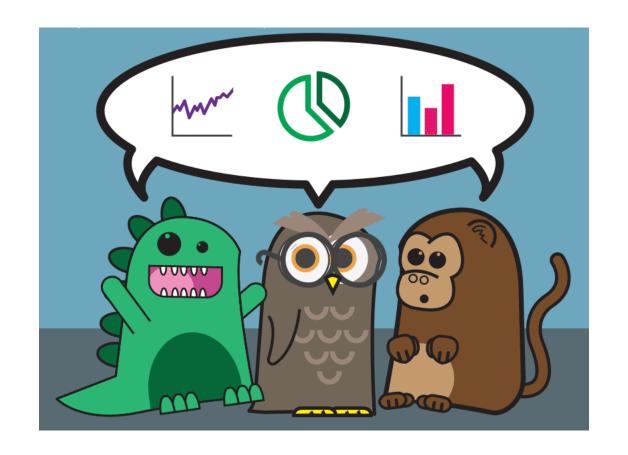GGC5039 / ESS419

Academic Communication

Section 4-2: Presentations at Conferences (Poster)

Instructor: Dikun Yang

Term: Fall 2020-2021
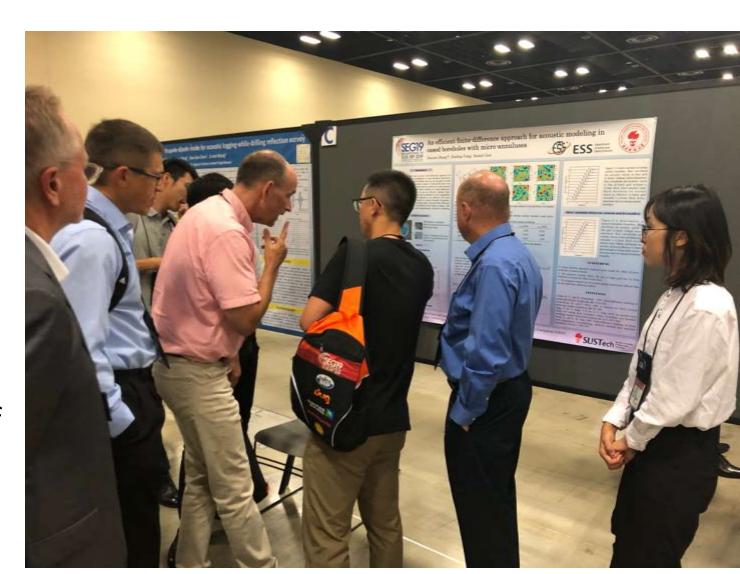
Outline

- Section 1: **Introduction** (2 hr)
- Section 2: **International communications** (2 hr)
- Section 3: **Writing and publishing** (8 hr) – Assignment 15%
- Section 4: **Presentations at conferences** (6 hr) – Assignment 15%
- Section 5: **Writing proposals and applications** (6 hr) – Assignment 15%
- Section 6: **Interviews** (4 hr) – Assignment 15%
- Section 7: **New media** (2 hr) – Assignment 15%
- Section 8: **Integrated practice** (2 hr) – Final defense/participation 25%

Poster Session

- Same submission/review procedure as oral
- Can be requested or can be assigned by chairs
- Sometimes considered less important than oral but not always
- Face-to-face and informal interaction
- Less restricted by time
- Suitable for topics with lots of technical details

Why Poster

- Good for first-time presenters/stage fright
- Good for complicated contents or multiple conclusions (a poster is two-dimensional)
- Good opportunities to meet and talk to people (future reviewers, employers, advisors, etc.)
- Good for other people to memorize you and your work (need good graphic design)
- Bring back and decorate your office

Style of Posters

- IMRAD: left-right or top-bottom
- Graphic: more figures than texts (500 ~ 1000 words)
- Bulleted/numbered list: avoid lengthy paragraphs
- Self-explanatory: in case you are not in front of your poster
- Highlights: like a short abstract
- Information about further contact or communication
- Less is more: avoid crowding
- Decent taste of coloring and design
- Font size: can be seen from 1 ~ 3 m away

Title of the Research Study

PEOPLE WHO DID THE STUDY

UNIVERSITIES AND/OR HOSPITALS THEY ARE AFFILIATED WITH

Introduction

We hope you find this template useful! This one is set up to yield a 48x72" (4x6') horizontal poster when we print it at 200%.

We've put in the headings we usually see in these posters, you can copy and paste and change to your hearts content! We suggest you use keep black text against a light background so that it is easy to read. Background color can be changed in format-background-drop down menu.

The boxes around the text will automatically fit the text you type, and if you click on the text, you can use the little handles that appear to stretch or squeeze the text boxes to whatever size you want. If you need just a little more room for your type, go to format-line spacing and reduce it to 90 or even 85%.

The dotted lines through the center of the piece will not print, they are for alignment. You can move them around by clicking and holding them, and a little box will tell you where they are on the page. Use them to get your pictures or text boxes aligned together.

How to bring things in from Excel® and Word®

Excel- select the chart, hit edit-copy, and then edit-paste into PowerPoint®. The chart can then be stretched to fit as required. If you need to edit parts of the chart, it can be ungrouped. *Watch out* for scientific symbols used in imported charts, which PowerPoint will not recognize as a used font and may print improperly if we don't have the font installed on our system. It is best to use the Symbol font for scientific characters.

Word- select the text to be brought into PowerPoint, hit edit-copy, then edit-paste the text into a new or existing text block. This text is editable. You can change the size, color, etc. in format-text. We suggest you not put shadows on smaller text. Stick with Arial and Times New Roman fonts so your collaborators will have them.

Scans

We need images to be 72 to 100 dpi in their final size, or use a rule of thumb of 2 to 4 megabytes of uncompressed .tif file per square foot of image. For instance, a 3x5 photo that will be 6x10 in size on the final poster should be scanned at 200 dpi.

We prefer that you import tif or jpg images into PowerPoint. Generally, if you double click on an image to open it in Microsoft Photo Editor, and it tells you the image is too large, then it is too large for PowerPoint to handle too. We find that images 1200x1600 pixels or smaller work very well. Very large images may show on your screen but PowerPoint cannot print them.

Preview: To see your in poster in actual size, go to view-zoom-100%. Posters to be printed at 200% need to be viewed at 200%.

Feedback: If you have comments about how this template worked for you, email to sales@megaprint.com.

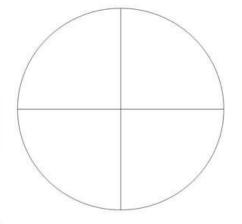We listen! Call us at 800-590-7850 if we can help in any way.

Methods

Xxxxxxxxxxxxxxxxxxxxxxxxxxxxxxxxxxxxxxxxxxxxxxxxxxxxx
xxxxxxxxxxxxxxxxxxxxxxxxxxxxxxxxxxxxxxxxxxxxxxxxxxxx
xxxxxxxxxxxxxxxxxxxxxxxxxxxxxxxxxxxxxxxxxxxxxxxxxxxx
xxxxxxxxxxxxxxxxxxxxxxxxxxxxxxxxxxxxxxxxxxxxxxxxxxxx
xxxxxxxxxxxxxxxxxxxxxxxxxxxxxxxxxxxxxxxxxxxxxxxxxxxx
xxxxxxxxxxxxxxxxxxxxxxxxxxxxxxxxxxxxxxxxxxxxxxxxxxxx
xxxxxxxxxxxxxxxxxxxxxxxxxxxxxxxxxxxxxxxxxxxxxxxxxxxx
xxxxxxxxxxxxxxxxxxxxxxxxxxxxxxxxxxxxxxxxxxxxxxxxxxxx
xxxxxxxxxxxxxxxxxxxxxxxxxxxxxxxxxxxxxxxxxx.

Yyyyyyyyyyyyyyyyyyyyyyyyyyyyyyyyyyyyyyyyyyyyyyyyyyyy
yyyyyyyyyyyyyyyyyyyyyyyyyyyyyyyyyyyyyyyyyyyyyyyyyyyy
yyyyyyyyyyyyyyyyyyyyyyyyyyyyyyyyyyyyyyyyyyyyyyyyYyy
yyyyyyyyyyyyyyyyyyyyyyyyyyyyyyyyyyyyyyyyyyyyyyyyyyyy
yyyyyyyxxxxxxxxxxxxxxxxxxxxxxxxxxxxxxxxxxxxxxxxxxxxx
xxxxxxxxxxxxxxxxxxxxxxxxxxxxxxxxxxxxxxxxxxxxxxxxxxxx
xxxxxxxxxxxxxxxxxxxxxxxxxxxxxxxxxxxxxxxxxxxxxxxxxxxx
xxxxxxxxxxxxxxxxxxxxxxxxxxxxxxxxxxxxxxxxxxxxxxxxxxxx
xxxxxxxxxxxxxxxxxxxxxxxxxxxxxxxxxxxxxxxxxxxxxxxxxxxx
xxxx.

Figure #1

CHART or PICTURE

Results

Xxxxxxxxxxxxxxxxxxxxxxxxxxxxxxxxxxxxxxxxxxxxxxxxxxxxx
xxxxxxxxxxxxxxxxxxxxxxxxxxxxxxxxxxxxxxxxxxxxxxxxxxxx
xxxxxxxxxxxxxxxxxxxxxxxxxxxxxxxxxxxxxxxxxxxxxxxxxxxx
xxxxxxxxxxxxxxxxxxxxxxxxxxxxxxxxxxxxxxxxxxxxxxxxxxxx
xxxxxxxxxxxxxxxxxxxxxxxxxxxxxxxxxxxxxxxxxxxxxxxxxxxx
xxxxxxxxxxxxxxxxxxxxxxxxxxxxxxxxxxxxxxxxxxxxxxxxxxxx
xxxxxxxxxxxxxxxxxxxxxxxxxxxxxxxxxxxxxxxxxxxxxxxxxxxx
xxxxxxxxxxxxxxxxxxxxxxxxxxxxxxxxxxxxxxxxxxxxxxxxxxxx
xxxxxxxxxxxxxxxxxxxxxxxxxxxxx

xxxxxxxxxxxxxxxxxxxxxxxxxxxxxxxxxxxxxxxxxxxxxxxxxxxx
xxxxxxxxxxxxxxxxxxxxxxxxxxxxxxxxxxxxxxxxxxxxxxxxxxxx
xxxxxxxxxxxxxxxxxxxxxxxxxxxxxxxxxxxxxxxxxxxxxxxxxxxx
xxxxxxxxxxxxxxxxxxxxxxxxxxxxxxxxxxxxxxxxxxxxxxxxxxxx
xxxxxxxxxxxxxxxxxxxxxxxxxxxxxxxxxxxxxxxxxxxxxxxxxxxx
xxxxxxxxxxxxxxxxxxxxxxxxxxxxxxxxxxxxxxxxxxxxxxxxxxxx
xxxxxxxxxxxxxxxxxxxxxxxxxxxxxxx

Figure #2

Conclusions

Xxxxxxxxxxxxxxxxxxxxxxxxxxxxxxxxxxxxxxxxxxxxxxxxxxxxx
xxxxxxxxxxxxxxxxxxxxxxxxxxxxxxxxxxxxxxxxxxxxxxxxxxxx
xxxxxxxxxxxxxxxxxxxxxxxxxxxxxxxxxxxxxxxxxxxxxxxxxxxx
xxxxxxxxxxxxxxxxxxxxxxxxxxxxxxxxxxxxxxxxxxxxxxxxxxxx
xxxxxxxxxxxxxxxxxxxxxxxxxxxxx

xxxxxxxxxxxxxxxxxxxxxxxxxxxxxxxxxxxxxxxxxxxxxxxxxxxx
xxxxxxxxxxxxxxxxxxxxxxxxxxxxxxxxxxxxxxxxxxxxxxxxxxxx
xxxxxxxxxxxxxxxxxxxxxxxxxxxxxxxxxxxxxxxxxxxxxxxxxxxx
xxxxxxxxxxxxxxxxxxxxxxxxxxxxxxxxxxxxxxxxxxxxxxxxxxxx
xxxxxxxxxxxxxxxxxxxxxxxxxxxxxxxxxxxxxxxxxxxxxxxxxxxx
xxxxxxxxxxxxxx

Bibliography

1. Xxxxxxxxxxxxxxxxxxxxxxxxxxxxxxxxxxxxxxxxxxxxx xxxxxxxxxxxxxxxxxxxxxxxxxxxxxxxxxxxxxxxxxx
2. Xxxxxxxxxxxxxxxxxxxxxxxxxxxxxxxxxxxxxxxxxxxxx xxxxxxxxxxxxxxxxxxxxxxxxxxxx
3. Xxxxxxxxxxxxxxxxxxxxxxxxxxxxxxxxxxxxxxxxxxxxx xxxxxxxxxxxxxxxxxxxxxxxxxxxxxxxxxxxxxxxxxxxxx xxxxxxxxxxxxxxxxxx
4. Xxxxxxxxxxxxxxxxxxxxxxxxxxxxxxxxxxxxxxxxxxxxx xxxxxxxxxxxxxxxxxxxxxxxxxxxxxxxxxxxxx

Title, name, affiliation, logo

I

M

R

D/C

Title, name, affiliation, logo

I

M

R

D/C

Inversion of E-field Time Domain EM Data

Dikun Yang, Douglas Oldenburg

Geophysical Inversion Facility · Department of Earth and Ocean Sciences · University of British Columbia
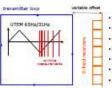
Introduction

Information about the electrical conductivity of the earth can be coded in the magnetic or electric fields arising from a geophysical survey. Typically only the magnetic field, or its time derivative, is interpreted when using inductive sources. Here we investigate the potential for using electric field (E-field) data. We illustrate the time domain E-field method by using the "Inductive Source Resistivity (ISR)" method, a ground EM survey proposed by Lamontagne Geophysics Ltd.

In this work we explain some basic aspects of the ISR method, including the sensitivity analysis and 3D synthetic forward modeling, and invert data from a synthetic example. We also invert field data from Shea Creek, a uranium deposit in Saskatchewan.

Configuration of ISR

Figure 1. Basic layout of ISR
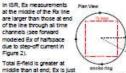
- Transmitter: non-grounded loop
- Receiver: dipole electrodes
- Dipole spacing: 25 or 50m
- Measurement: Ex (inline)
- Waveform: UTEM triangular
- Base frequency: 65 or 31Hz
- Time channel: 20 (UTEM)

Responses of ISR

Time varying magnetic fields from the transmitter induce secondary currents in the ground. These diffuse outwards from the transmitter and are often thought of as "smoke rings". Electric fields are generated by eddy currents in a conductor and also by galvanic currents which give rise to electric charges at an interface of conductivity contrast.

Horizontal Distribution of E-field

In ISR, Ex measurements at the middle of the Rx line are larger than those at end of the line through all time channels (see forward modeled Ex of halfspace due to step-off current in Figure 2).

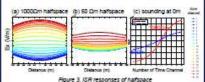Total E-field is greater at middle than at end; Ex is just one component of total E-field off the middle sounding.

Figure 2. E-field along a survey line

ISR Responses of Halfspace

- Ex changes sign as the current in transmitter loop goes from negative to positive during and after the last 1/4 period.
- A conductive ground results in a smaller dynamic range of Ex (see Figure 3c), which is an important indicator of conductor in ISR.

Figure 3. ISR responses of halfspace

ISR Responses of Conductive and Resistive Prisms

The forward modeled responses for a conductive and resistive prism are shown in Figure 4.

- Large-scale features: caused by the halfspace background conductivity.
- Local-scale features: dynamic range of Ex shrinks or inflates at the place where the conductor or resistor is found.
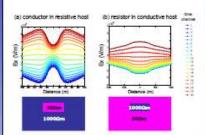

Figure 4. ISR responses of conductor and resistor

Sensitivity of ISR

Sensitive Region of ISR Survey

An inversion-based method to find the 3D region contributing to the Ex measurements (see isosurface in Figure 6):

(1) Compute synthetic data. The conductivity model is a 100Ωm half-space. The survey layout and numerical modeling mesh are shown in Figure 5.

(2) Invert the data with a starting model and reference model of 100Ωm. Cells that have conductivities different from the reference model are considered to be responsible for the observed data.
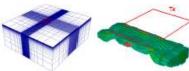

Figure 5. Forward modeling of 100Ωm halfspace

Figure 6. Recovered sensitive cells

Figure 7. Cross section of sensitive region

- The sensitive region is primarily between Tx loop and Rx line.
- The bottom of this region is about 400~500m at depth.
- The blue colored cells are close to reference model, so they are relatively insensitive (Figure 7).

Detectability of Deep Weak Conductor

Because of small eddy currents, a deep weak conductor may not be sensed well by magnetic field data. However, E-field data might be relatively strong if enough charges are built up on conductivity contrast. A forward modeling test quantitatively shows a better sensitivity of Ex than dBz/dt to detect such a target.
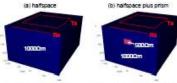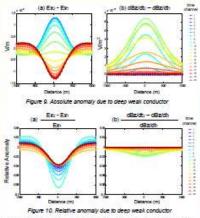

Figure 8. Forward modeling of Ex and dBz/dt for halfspace and prism

- Forward model Ex and dBz/dt for 100Ωm halfspace (Figure 8a); Ex and dBz/dt soundings are coincident.
- Forward model Ex and dBz/dt for a model of 100Ωm halfspace plus 500Ωm conductor below ~400m (Figure 8b).

The absolute and relative anomalies caused by the conductive prism are shown in Figure 9 and 10 respectively.

Figure 9. Absolute anomaly due to deep weak conductor

Figure 10. Relative anomaly due to deep weak conductor

- An object can be detected if the absolute and relative anomalies are sufficiently large. This depends upon the instrument and ambient noise level.
- The Ex data show at least a 4% anomaly for all time channels for deep prism. The relative anomaly of dBz/dt may be easily disturbed by 1%~2% noise (Figure 10).
- E-field TEM may be especially helpful for the exploration of poorly or intermediately conductive targets or in cases where the magnetic field based method does not work well due to weak signal or magnetic noise.

3D Inversion of Synthetic Model

The inversion algorithm is that outlined by Haber, Oldenburg, and Shekhtman, 2007. A test inversion of a synthetic model was carried out to evaluate the code's capability of inverting E-field data. The model, a 100Ωm background and a 50Ωm prism, simulates an alteration zone buried in sandstone background (Figure 11). A ISR data set for one loop was forward modeled (Figure 12).
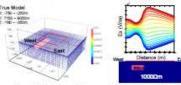

Figure 11. Synthetic model

Figure 12. Synthetic ISR data

A 100Ωm halfspace was used as an initial and reference model. Data misfit converged to target misfit (chifact = 1) after 14 iterations (Figure 13). The final model perfectly reproduced the observed data (Figure 14). Comparing the recovered model to the true model (Figure 15 and 16), it is obvious that the inversion correctly delineated part of the prism under or near the Rx line.
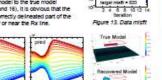

Figure 13. Data misfit

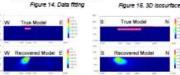Figure 14. Data fitting

Figure 15. 3D isosurface

Figure 16. Cross sections of final inversion model
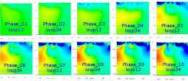
3D Inversion of ISR Field Data

An ISR dataset was acquired with the configuration shown in Figure 17 and Table 1. The goal was to search for uranium at the Shea Creek deposit, Saskatchewan.
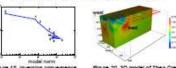
Table 1. Parameters of Shea Creek ISR

Tx	Rx	Offset	Freq	Spacing
Loop 1	7200N	400m	65Hz	25m
Loop 2	7200N	800m	65Hz	25m
Loop 3	7200N	1200m	31Hz	50m
Loop 4	7200N	1600m	31Hz	50m

Figure 17. Shea Creek ISR survey

Two different waveforms were used. We split the whole dataset into two parts, loop12 and loop34, and inverted them alternately with an iterative Tikhonov approach. That is, invert loop12, then loop34, then loop 12 etc. The inversion model from the previous phase was used as a reference and initial model for the next inversion. The tradeoff parameter was continually decreased. The procedure continued until the total misfit could not be reduced. (see Figure 18 for evolution of inversion model; see Figure 19 for convergence of data misfit)

Figure 18. Cross sections at 7200N in each inversion phase

Figure 19. Inversion convergence

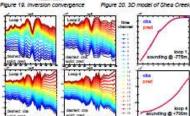

Figure 20. 3D model of Shea Creek
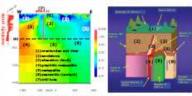

Figure 21. Shea Creek ISR data fitting

Figure 22. Cross section at 7200N and geologic interpretation

Figure 20 shows the 3D inversion model that acceptably fits the observed ISR data (Figure 21). A cross section of the conductivity model at 7200N is geologically interpreted with in accordance with the exploration model built up by the previous works (Figure 22).

Conclusions

- E-field data from inductive sources (ISR data) can be 3D inverted.
- Field data inversion produces features that have a geologic interpretation.
- More data could improve the resolution and better constrain 3D inversion.

Bibliography

Haber, E., Oldenburg, D. W., Shekhtman, R., 2007, Inversion of time domain three-dimensional electromagnetic data, Geophys. J. Int., 171.
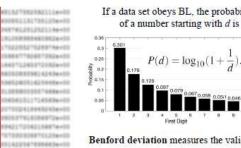
THE UNIVERSITY OF BRITISH COLUMBIA
DIKUN YANG
yangdikun@gmail.com

Characterization of noise in airborne transient electromagnetic data using Benford's law

- Benford's law: how often 1 to 9 appear as the first digit of numbers in a data set.
- Actual geophysical data obey Benford's law, while a random noise does not.
- Deviation from the ideal Benford's frequency can indicate the level of random noise.
- A trivial and fast approach to probe a large data set and estimate the noise.

Benford's law (BL): Only the first digits matter (Benford, 1938).

If a data set obeys BL, the probability of a number starting with d is

$$P(d) = \log_{10}\left(1 + \frac{1}{d}\right).$$

- Contains many numbers
- Spans many orders of magnitude
- In log-uniform distribution
- Hydrological data (Nigrini and Miller, 2007)
- Earthquake data (Sambridge et al., 2010).

Benford deviation measures the validity of BL for a data set

$$\delta = \sqrt{\sum_{d=1}^{9}\left[\frac{F(d) - P(d)}{P(d)}\right]^2},$$
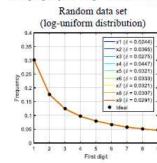
$P(d)$: the ideal Benford frequency
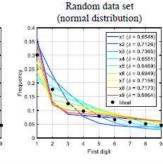$F(d)$: the evaluated Benford frequency

Scale invariance
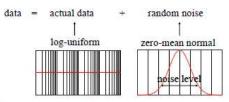$F(d)$ does not change if the data are multiplied by an arbitrary constant. This property offers great convenience in raw data analysis.

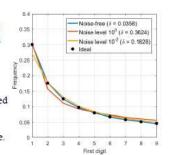Random data set (log-uniform distribution)

Random data set (normal distribution)

Test on synthetic data sets

data = actual data + random noise

log-uniform   zero-mean normal

Three synthetic data sets:

- **Noise-free**: actual data are random numbers in log-uniform distribution between 10^{-2} and 10^2.
- **Noise level 10^0**: the noise-free data plus a noise in a normal distribution of unity standard deviation.
- **Noise level 10^{-2}**: the noise-free data plus a noise in a normal distribution of 10^{-2} standard deviation.

At a higher noise level, more actual data are swamped by the noise, so more noise are included in the calculation of δ. δ can be considered as a *relative* measure of the noise's dominance.
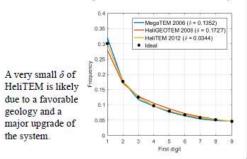

Test on real data sets

Three airborne transient EM (ATEM) data sets acquired by Fugro (now CGG) with similar electronics:

- MegaTEM (2006): a fixed-wing system, base frequency 90 Hz, transmitter moment 1.49 million Am^2, number of data 468877, at a uranium site.
- HeliGEOTEM (2008): a helicopter system, base frequency 30 Hz, transmitter moment 0.8 million Am^2, number of data 824720, at a porphyry site.
- HeliTEM (2012): a helicopter system, base frequency 30 Hz, transmitter moment 1.9 million Am^2, number of data 781303, at a volcanogenic massive sulphide.

All data sets reasonably obey BL with small δ's.
The actual data are dominant over the noise.
A more controlled experiment is desired in future study.

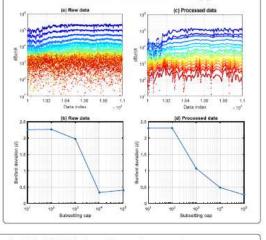A very small δ of HeliTEM is likely due to a favorable geology and a major upgrade of the system.

Estimation of absolute noise level

Infer the absolute noise level using the information from the exponents and a dynamic subsetting method:

- Trials with an increasing subsetting cap.
- Only the numbers below the cap are analyzed for δ.
- The δ curve as a function of the cap is diagnostic.

Two version of the MegaTEM (2006) data sets:

- Raw in high noise (a): sharp reduction of δ as the cap excesses the noise level (b).
- Processed in low noise (c): gradual reduction of δ as more data are included in the calculation (d).

Conclusions

- A "random noise" in "actual data" of certain types can be distinguished by BL using only the first digits.
- The simplicity of BL and its scale invariance make it promising in fast analysis of raw data in large amount.
- BL is effective in estimating the relative noise level in airborne TEM data. With additional information from the exponents, the absolute noise level can be inferred.

Links

SEG Expanded Abstract
DOI:10.1190/segam2016-13972000.1

Benford Online Bibliography
An online bibliographic database on the theory and applications of BL
http://www.benfordonline.net

- Benford, F., 1938, The law of anomalous numbers: *Proceedings of the American Philosophical Society*, 551–572.
- Nigrini, M. J., and S. J. Miller, 2007, Benford's law applied to hydrology data results and relevance to other geophysical data: *Mathematical Geology*, 39, 469–490.
- Sambridge, M., H. Tkalčić, and A. Jackson, 2010, Benford's law in the natural sciences: *Geophysical Research Letters*, 37.

The real data sets were courtesies of Fugro (now CGG), Cameco and Terrane Metals (now Thompson Creek Metals).

Nabighian's Smoke Rings in 3D Inversion

Dikun Yang *Southern University of Science and Technology, Shenzhen, China*
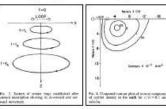**Douglas W. Oldenburg** *University of British Columbia, Vancouver, Canada*
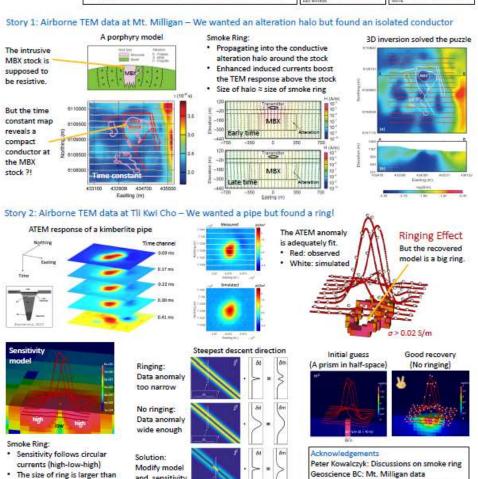
The concept of "smoke ring", developed by Nabighian with a uniform half-space in the 70's, is such a profound and intuitive model that we still cannot get away with in today's 3D inversion. This poster presents two research stories of our own to show the influence of Nabighian's early work on modern geophysical technology.

SMOKE RING
A puff of smoke that has been "blown by the transmitter loop"

Story 1: Airborne TEM data at Mt. Milligan – We wanted an alteration halo but found an isolated conductor

A porphyry model

The intrusive MBX stock is supposed to be resistive.

But the time constant map reveals a compact conductor at the MBX stock ?!

Smoke Ring:
* Propagating into the conductive alteration halo around the stock
* Enhanced induced currents boost the TEM response above the stock
* Size of halo ≈ size of smoke ring

3D inversion solved the puzzle

Story 2: Airborne TEM data at Tli Kwi Cho – We wanted a pipe but found a ring!

ATEM response of a kimberlite pipe

The ATEM anomaly is adequately fit.
* Red: observed
* White: simulated

Ringing Effect
But the recovered model is a big ring.

$\sigma > 0.02$ S/m

Sensitivity model

Smoke Ring:
* Sensitivity follows circular currents (high-low-high)
* The size of ring is larger than the width of anomalous data

Steepest descent direction

Ringing:
Data anomaly too narrow

No ringing:
Data anomaly wide enough

Solution:
Modify model and sensitivity

Initial guess
(A prism in half-space)

Good recovery
(No ringing)

Rheo-Physics of Shear Thickening Fluids during Large Amplitude Oscillatory Shear (LAOS)

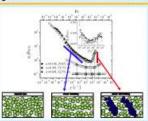A. Kate Gurnon[1], John W. Gillespie Jr.[2] and Norman J. Wagner[1]
[1]University of Delaware Chemical Engineering Department and [2]Center for Composite Materials

Motivation

Shear Thickening Fluids (STFs) are concentrated colloidal suspensions that exhibit increases in viscosity under high shear rates of deformation. Recent research has moved toward exploiting the exceptional damping properties of STFs for use in applications such as personal protective armor. This application motivates a more fundamental understanding of the nonlinear rheological response of STFs.
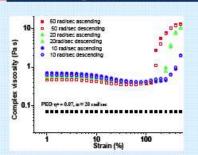
Our objectives are two fold:
I. To present measurements of shear thickening fluids (STFs) under large amplitude oscillatory shear (LAOS) conditions.
II. To develop a way to use LAOS measurements to determine the nonlinear parameter of a constitutive equation that will be used to model the shear thinning regime of a STF

Model STF system (500nm diameter silica particles in PEG-200) during steady shear deformation highlighting the shear thinning and shear thickening regimes from D.P. Kalman and Wagner, N.J. *Rheologica Acta*, 2009. 48(8). 897-908.
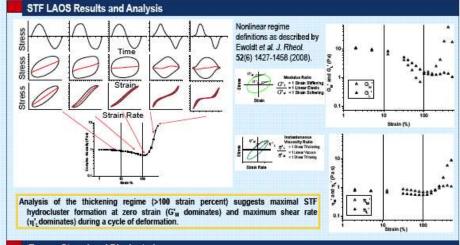
Part I: STF During LAOS Deformation

- 50 rad/sec ascending
- 50 rad/sec descending
- 20 rad/sec ascending
- 20rad/sec descending
- 10 rad/sec ascending
- 10 rad/sec descending

PEG $\eta_\infty = 0.07$, $\alpha = 20$ rad/sec

Suspension:
47 volume percent silica particles (500nm diameter) in PEG-200
Test Conditions:
T = 20 C

STF LAOS Results and Analysis

Nonlinear regime definitions as described by Ewoldt et al. *J. Rheol.* 52(6) 1427-1458 (2008).

Modulus Ratio
$\frac{G'_L}{G'_M}$ > 1 Strain Stiffening
= 1 Linear Elastic
< 1 Strain Softening

Instantaneous Viscosity Ratio
$\frac{\eta'_L}{\eta'_M}$ > 1 Shear Thickening
= 1 Linear Viscous
< 1 Shear Thinning

Analysis of the thickening regime (>100 strain percent) suggests maximal STF hydrocluster formation at zero strain (G'_M dominates) and maximum shear rate (η'_L dominates) during a cycle of deformation.

Energy Stored and Dissipated

Nonlinear stress response in Fourier Space:

$$\tau = \sum_{n=1}^{\infty} \tau_n^* e^{in\omega t} = \sum_{n=1}^{\infty} [(A_n + iB_n)\cos(n\omega t) + (-B_n + iA_n)\sin(n\omega t)]$$

$$\dot{E} = \oint \tau : 2\mathbf{D}(t)dt$$

We observe the energy dissipated is always larger than the energy stored and both increase significantly in the thickening regime suggesting STFs exhibit both stiffening and dampening qualities.
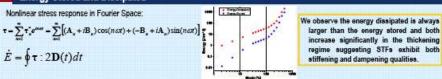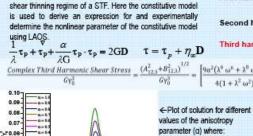
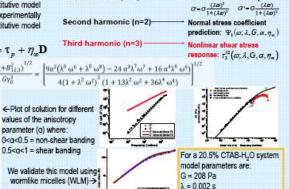## Part II: Extracting a Nonlinear Constitutive Equation Parameter using LAOS

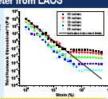The Giesekus constitutive equation will be used to model the shear thinning regime of a STF. Here the constitutive model is used to derive an expression for and experimentally determine the nonlinear parameter of the constitutive model using LAOS.

$$\frac{1}{\lambda}\tau_P + \tau_P + \frac{\alpha}{\lambda G}\tau_P \cdot \tau_P = 2\mathbf{GD} \qquad \tau = \tau_p + \eta_\infty \mathbf{D}$$

$$\frac{Complex\ Third\ Harmonic\ Shear\ Stress}{G\gamma_0^3} = \frac{(A_{12,3}^2 + B_{12,3}^2)^{1/2}}{G\gamma_0^3} = \left[\frac{9\alpha^2(\lambda^6\omega^6 + \lambda^8\omega^8) - 24\alpha^3\lambda^7\omega^7 + 16\alpha^4\lambda^6\omega^6}{4(1+\lambda^2\omega^2)^3(1+13\lambda^2\omega^2+36\lambda^4\omega^4)}\right]^{1/2}$$

First harmonic (n=1) — Linear shear stress response:
$$G' = G\frac{(\lambda\omega)^2}{1+(\lambda\omega)^2} \qquad G'' = G\frac{(\lambda\omega)}{1+(\lambda\omega)^2}$$

Second harmonic (n=2) — Normal stress coefficient prediction: $\Psi_1(\omega;\lambda,G,\alpha,\eta_\infty)$

Third harmonic (n=3) — Nonlinear shear stress response: $\tau_3^{12}(\omega;\lambda,G,\alpha,\eta_\infty)$

← Plot of solution for different values of the anisotropy parameter (α) where:
0<α<0.5 = non-shear banding
0.5<α<1 = shear banding

We validate this model using wormlike micelles (WLM) →

For a 20.5% CTAB-H$_2$O system model parameters are:
G = 208 Pa
λ = 0.002 s
η_∞ = 0.006 Pa s
α = 0.41

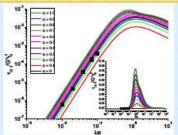## Anisotropy Parameter from LAOS

LAOS measures the third harmonic stress contribution at five different frequencies.

Using the third harmonic stress contributions we solve for the anisotropy parameter (α). Plotting these (black points) we see the solution from the third harmonic corresponds with the α=0.4 analytical solution.

Conclusions

We conclude the shear stress response of STFs under LAOS has a highly nonlinear response and can be understood within the context of the analysis used here. The results suggest maximal STF hydrocluster formation occurs at zero strain and maximum shear rate.

We have evaluated the Giesekus model for nonlinear shear responses and derived an expression to find the anisotropy parameter from a LAOS measurement.

Future Work

- Image STF dynamic responses during LAOS using time resolved Small Angle Neutron Scattering (t-SANS) under oscillatory shear.
- Implementation of a multi-mode version of the Giesekus constitutive model for use in modeling the shear thinning behavior in a STF.

Research Funding and Contact Information

A. Kate Gurnon – akgurnon@udel.edu
Univ. of Delaware Chemical Engineering Department
www.che.udel.edu
150 Academy Street
Newark, DE 19716

Assets Reconsidered: Alternative Assets and Fathers' Well-being

Kimberly J. Turner
University of Wisconsin-Madison

THE UNIVERSITY WISCONSIN MADISON

Center for Demography and Ecology

Background/Conceptual Framework

- Accumulated assets function much like a storehouse supporting incoming flows of resources.

- With limited reserves, one is in a precarious position, wholly dependent on the current in-flow of resources – a position all too familiar to low-income fathers.

- Possessing few traditional financial assets (i.e., savings, value of an owned home, stocks and bonds), disadvantaged individuals invoke survival strategies, often relying on personal safety nets (Edin & Lein 1997; Edin & Lein 1997b; Anderson 1999).

- Survival strategies reflect various forms of alternative assets – resources that represent ranging dimensions of human, cultural, social, organizational, and political capital – that help individuals meet their basic needs (Sherraden 1991; Sharpiro & Wolff 2001).

- Acquisition and maintenance of alternative assets require investments of time and energy (Dominguez & Watkins 2003; Nelson 2000).

Research Question

What is the relationship between fathers' social support/engagement and fathers' physical, mental, and economic well-being?

Data

- Fragile Families and Child Well-being Study (PIs: McLanahan & Garfinkel)
- Longitudinal study of urban birth cohort of 4,897 births between 1998 and 2000
- Twenty U.S. cities of population 200k+
- Over-sample of nonmarital births (3,710) with comparison group of marital births (1,187)
- Follow-up interviews occurred approximately 1, 3 and 5 years after child's birth

Analytic Sample and Methods

Analytic Sample

- Both marital and nonmarital births
- Interviewed fathers only (about 4/5 of births)
  - Interview did not occur in jail
  - Child lived with biological mother
- Separate analyses of resident and non-resident fathers: 1Yr – 85% resident; 5Yr – 72% resident
- Number of cases = 3,775 unique fathers
  → 8,845 person – year observations (5,960 Resident; 2,885 Non-Resident)

Methods

- Examine fathers' well-being and social support/engagement at years 1, 3 and 5
- Using pooled data across years with time-varying residence status
- Estimate separate models by residence status
- Random effects models (both between- and within-father differences)
- Fixed effects models (only within-father differences)

Fathers' Social Support and Engagement

Perceived Instrumental Support (Range = 0-6)

- Can count on someone to: (a) loan $200, (b) loan $1000, (c) provide a place to stay, (d) provide emergency childcare, (e) co-sign a $1000 loan (f) and co-sign a $5000 loan.
- Summed Scale (α > .70 for resident fathers; α > .70 for non-resident fathers)

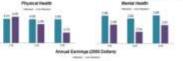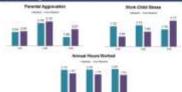**Received Financial Support from family and friends (in 1000s)**

- Inflation-adjusted amount of financial support received from family and friends.

Social Engagement (1YR)	Resident %	Non-Resident %
Participate in an Community Organization	50.8	50.7
Participate in a Protest	10.4	10.1
Registered to Vote	72.5	81.4
Voted in Presidential Election	74.5	61.3

Fathers' Well-being

Key Baseline Demographics and Control Variables

Residence Status at 1 Year	Resident	Non-Resident
Race/ethnicity		
White non-Hispanic	32.3	9.3
Black non-Hispanic	27.78	64.4
Hispanic	34.1	20.2
Education		
Less than HS	28.9	31.2
HS degree	32.1	39.7
Some college	22.8	17.9
College degree	15.2	3.1
Married to child's mother	36.8	3.1

Note: Weighted by city sampling weights.

Control Variables	
Time Constant	**Time-Varying**
Age at child's birth	Fathers' involvement
Foreign born	Relationship with biological mother
Lived with parents at 15	Fathers' education
Depressive symptoms (CES-D)	Grandmother coresiding with child
Self-reported health	Mothers' hours worked per week
Religious service attendance	Relationship status
Positive fathering attitudes	- Married
Has previous child w/ other partner	- Dating
Number of children w/ bio mother	- New Partner

Results

	Social Support				Social Engagement					
	Perceived Support		Received Support		Religious Service Attendance		Comm Org	Part. Protest	Reg. Vote	Vote Prez
	RE	FE	RE	FE	RE	FE	RE	RE	RE	RE
Resident Fathers										
Physical Health	.051**	.038**	-.003	-.001	.011	.004	.030	-.020	-.023	.034
Mental Health	.021**	.017**	-.003*	.000	.016**	-.007	.009	-.084*	.012	.022
Parental Stress	-.027**	-.003	-.000	-.003	-.016*	-.018*	-.062*	-.041	-.069*	.026
Work-Child Stress	-.051**	-.039**	.005	.002	-.003	.001	-.030	.059	-.076*	-.047*
Annual hours worked (ln)	.047**	.029**	-.007*	-.004	.014*	.004	.021	.005	.067*	.044
Annual earnings (ln)	.078**	.028**	-.002	-.001	.000	.000	.017	-.020	.064	.041
Non-Resident Fathers										
Physical Health	.075**	.036*	-.005	-.004	.036**	.057*	.009	-.296	-.058	-.008
Mental Health	.027**	.019*	-.019**	-.022**	.026**	.012	.023	-.096	.079*	.118**
Parental Stress	-.029**	-.031*	-.003	.012	-.020*	-.014	-.058	.029	-.037	-.026
Work-Child Stress	-.041**	-.039*	-.010	-.025*	-.035**	-.050*	.001	.025	-.033	.051
Annual hours worked (ln)	.054**	.020	-.024*	.019	.011	.000	.069*	-.001	.115*	.096*
Annual earnings (ln)	.082**	.014	-.017	-.018	.033	.050	.025	-.110	.232*	.154**

Note: +p<.10 *p<.05 **p<.01

Summary of Findings

- **Resident fathers:**

  - Consistent positive (but modest) relationship between perceived social support and fathers' physical, mental and economic well-being.
    - Associated with lower levels of stress
    - A one-unit increase in perceived support is associated with a 3% increase in the average annual hours worked and earnings for resident fathers.

  - Negative relationship between received financial support and fathers' physical, mental and economic well-being in random effects models.

  - Attending religious services, participating in a community organization and being registered to vote are associated with lower levels of parental stress.

- **Non-resident fathers:**

  - Increasing perceived support is linked to better health and mental health outcomes (lower levels of stress).

  - Receiving financial support is associated with declines in mental health and increased work-child stress.

  - Participating in a community organization, being registered to vote and voting in a presidential election are all positively related to labor force attachment.

  - Those who registered to vote and voted in a presidential election have higher annual earnings and better mental health on average.

- Overall, the relationship between fathers' social support and engagement on fathers' well being is relatively consistent across residential contexts.

Next Steps / Limitations

Next Steps

- Examine the relationship between other types of alternative assets and fathers' well-being.
- Construct an aggregate measure of alternative assets

Limitations

- Interviewed fathers cannot be used to generalize to all fathers ('worst off' fathers are under-represented)
- Cannot disentangle directionality in the associations
- Unobserved heterogeneity

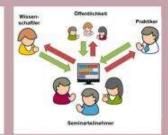## Acknowledgements

Transdisziplinäres Lernen in Wikis

Oliver Tacke

Technische Universität Braunschweig | Institut für Organisation und Führung

o.tacke@tu-braunschweig.de | Telefon +49 (0) 531 391-3642

Überblick

Während häufig in voneinander getrennten Umgebungen gelernt wird (Schulen, Universitäten, Betrieben, usw.), bedarf es in **einer modernen Gesellschaft** eines übergreifenden Austauschs als Quelle neuen Wissens – die Vernetzung untereinander gewinnt an Bedeutung. Hierzu wird insbesondere im Hochschulbereich dem **transdisziplinärem Lernen** zwischen Studierenden, Wissenschaftlern und Praktikern ein hohes Potenzial zugeschrieben. Gleichsam besteht durch eine **Öffnung nach außen** die Möglichkeit, weitere Teile der Bevölkerung an den Lernprozessen teilhaben zu lassen, nicht nur passiv als Empfänger sondern auch aktiv als Beitragende. Wegen der inhärenten Partizipationsmöglichkeiten in **sozialen Medien** liegt deren Einsatz nahe.

Im Sommersemester 2010 wurde im Fach Betriebswirtschaftslehre der Frage nachgegangen, ob sich bereits mit vergleichsweise geringem Aufwand transdisziplinäres Lernen durch Seminare in öffentlichen Wikis unterstützen lässt. Zusätzlich wurde ein Meinungsbild der Studierenden eingeholt.

Vorgehen

Die Studierenden sollten gruppenweise innerhalb eines **öffentlichen Wikis** Seminararbeiten anfertigen. Um die Wahrscheinlichkeit zu erhöhen, dass Außenstehende von sich aus auf das Seminar aufmerksam werden, wurde für den Kurs ein möglichst prominentes Wiki gesucht. Er wurde schließlich in der „Wikiversity" angelegt und dort beworben: http://de.wikiversity.org/wiki/Kurs:Teams_SoSe10. Die Wikiversity ist ein Schwesterprojekt der bekannten Wikipedia und stellt ein öffentliches Wiki zum **gemeinschaftlichen Lernen und Lehren** dar.

Die Studierenden wurden ermuntert, für ihr jeweiliges Thema Spezialisten zur Mitarbeit zu bewegen. Zusätzlich wurde der Kurs in verschiedenen Fachgruppen der sozialen Plattform XING vorgestellt und um Beteiligung gebeten. Ergänzend machte der Dozent mehrfach über sein Konto beim Microblogging-Dienst Twitter auf das Seminar aufmerksam und kontaktierte einen ihm bekannten Experten direkt.

Das Meinungsbild der Studierenden wurde nach Abschluss des Seminars per Fragebogen festgehalten und mittels einer Likert-Skala erfasst.

Website des Kurses in der Wikiversity

http://de.wikiversity.org/wiki/Kurs:Teams_SoSe10

Ergebnisse und Diskussion

Lediglich ein Interessent stieß spontan auf den Kurs und äußerte den Wunsch, daran selbst teilzunehmen. Mangels der Möglichkeit, dafür einen formellen Nachweis zu erhalten, sagte er jedoch ab. Weitere **Expertenbeteiligung von außen** erfolgte in Form von Literaturhinweisen und Interviews. Die getätigten Anstrengungen (möglichst bekannte Plattform, gezielte Werbung in Fachforen und Streuung über Twitter) genügten nicht, um übermäßig große Beteiligung Außenstehender zu erzeugen.

Die Mehrheit der Studierenden sieht in Wikis allgemein ein **praktisches Werkzeug**, um darin gemeinsam Arbeiten zu erstellen. Auch sehen sie es grundsätzlich positiv, dass Außenstehende sich mit ihren Ideen beteiligen können – die wenigsten haben allerdings wertvolle Beiträge erhalten. Folglich sehen sie es nur begrenzt als hilfreich an, dass weltweit jeder den Stand der Arbeit einsehen kann. Einige äußerten diesbezüglich gar etwas „Unwohlsein". Insgesamt stehen die Lernenden den öffentlichen Seminaren aber **positiv** gegenüber. Etwaige Bedenken sollten zu Beginn diskutiert werden.

Literatur

- **Faulstich, P. (Hrsg.) (2006):** *Öffentliche Wissenschaft*, Bielefeld.
- **Gibbons, M. et al. (2009):** *The new production of knowledge*, London.
- **Spannagel, C.; Schimpf, F. (2009):** *Öffentliche Seminare im Web 2.0*, in: Schwill, A.; Apostolopoulos, N. (Hrsg.): Lernen im Digitalen Zeitalter. Workshop-Band. Dokumentation der Pre-Conference zur DeLFI, Berlin, S. 13-20.
- **Tacke, O. (2010):** *Open Science 2.0: How Research and Education can benefit from Open Innovation and Web 2.0*, in: Bastiaens, T.; Baumöl, U.; Krämer, B. J. (Hrsg.): On Collective Intelligence, Berlin, Heidelberg, New York, S. 37-48.
- **Tacke, O.; Hobus, B. (2010):** *Learning to integrate knowledge: experiences with public wikis in academic seminars*, in: Learning Technology, 12. Jg., Nr. 3, S. 21-23.

Records of Migration and Ebb-Delta Breaching at Historic and Ancient Tidal Inlets along a River-Fed Paraglacial Barrier Island

Christopher J. Hein[1] (hein@vims.edu), Gregory Fitzsimons[2], Duncan FitzGerald[3], Andrew Fallon[1,4]

[1]Department of Physical Sciences, Virginia Institute of Marine Science, College of William and Mary, Gloucester Point, VA, USA; [2]Graduate School of Education, University of Massachusetts, Lowell, Lowell, MA, USA; [3]Department of Earth and Environment, Boston University, Boston, MA, USA; [4]ESS Group, Waltham, MA, USA

1. Motivation: Tidal Inlets in the Stratigraphic Record

Tidal inlets in the coastal system:
- Channels maintained by tidal flow which hydraulically connect backbarrier environments with the coastal ocean
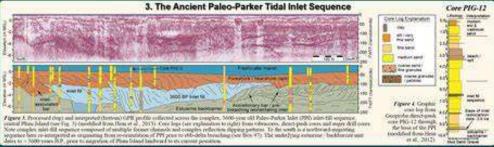- Among the most dynamic and ephemeral features of barrier systems
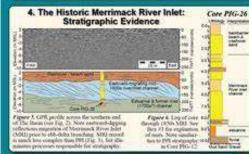
Tidal inlets in the stratigraphic record:
- Inlet-fill sequences comprise up to 50% of barrier lithosomes in wave-dominated settings (Moslow & Tye, 1985); commonly imaged with ground-penetrating radar (GPR) & sediment cores
- Also identified along shallow continental shelves & in rock record

Scientific Problem:
- Linking inlet-fill sequences to responsible erosional-depositional processes is largely inferential, based on observational studies at systems without direct relationships to ancient inlet-fills

2. Study Area: Plum Island, Gulf of Maine, USA

Figure 1. Location of study site (Plum Island) along the paraglacial (deglaciated ~17 kyr B.P.) coast of western Gulf of Maine, Mass., USA. (courtesy E. Hein)

Data Collection

Coastal Setting
- Island within the longest continuous barrier chain in the Gulf of Maine
- Mixed-energy, tide-dominated (range: 2.7 m)
- Northern end: Merrimack River mouth
- Influenced by strong northeast winter storms; dominant southerly long-shore sediment transport

Figure 2. A) Study area overview. B) Northern Plum Island. C) Central Plum Island and Parker River.

3. The Ancient Paleo-Parker Tidal Inlet Sequence

Core PIG-12

Figure 3. Processed (top) and interpreted (bottom) GPR profile collected across the complex, 5600-year old Paleo-Parker Inlet (PPI) inlet-fill sequence, central Plum Island (see Fig. 3) (modified from Hein et al., 2015). Core logs (see explanation to right) from vibracores, direct-push cores, and auger drill cores. Note complex inlet-fill sequence composed of multiple former channels and complex reflection dipping patterns. To the south is a northward-migrating sequence here re-interpreted as originating from re-orientation of PPI prior to ebb-delta breaching (see Box #7). The underlying estuarine / backbarrier unit dates to ~3600 years B.P., prior to migration of Plum Island landward to its current position.

Figure 4. Graphic core log from Geoprobe direct-push core PIG-12 through the basal of the PPI (modified from Hein et al., 2012)

4. The Historic Merrimack River Inlet: Stratigraphic Evidence

Core PIG-26

Figure 5. GPR profile across the northern end of The Basin (see Fig. 2). Note eastward-dipping reflections migration of Merrimack River Inlet (MRI) prior to ebb-delta breaching. MRI record is much less complex than PPI (Fig. 3), but illustrates processes responsible for stratigraphy.

Figure 6. Log of core through 1850s MRI. See Box #3 for explanation. Note similarities to PPI stratigraphy in Core PIG-12.

5. The Historic Merrimack River Inlet: Historic Evidence

Figure 7. Historic maps (top) and sketches of shorelines changes (bottom) at the MRI over a 150-year period. Data sources: Mitchell (1741); Desbarres (1741); Blunt (1809); Anderson (1826); Anderson (1830); US Coast Survey (1851); USACE (1883).

- Multiple phases of SW inlet migration & erosion of NE Plum Island shoreline
- Multiple developments of The Basin & NE fork of island (Old New Point)
- Migration halted by jetty installation (1880s)

6. Traditional Model: Ebb-Delta Breaching

- Erosion of NE Plum Island by southerly migrating MRI
- Inlet becomes hydraulically inefficient and breaches ebb-delta to create more direct (E-W) route
- Remnant ebb delta migrates onshore & welds to form New Point

Figure 8. Conceptual model of ebb-delta breaching at the MRI. Modified from FitzGerald (1993).

7. Ancient & Historic Inlets: Insights into the Stratigraphic Record

- Updated model of MRI evolution (Fig. 9): SW & landward-migrating MRI reoriented seaward in response to deflection by a protruding shoreline formed from the onshore welding of downdrift ebb-delta sediment
- Ebb-delta breaching more complex than traditional model
- Re-evaluation needed of details & complexities observed in stratigraphic (GPR, sediment cores) record? (example: see PPI sequence, Fig. 3)
- Comparison of historic & ancient inlet sequences underscores need to carefully document complex inlet processes recorded in inlet-fill sequences at close comparison with those preserved by modern analogs.

Figure 9. Updated model of MRI ebb-delta breaching based on Boxes 4&5.

8. References

FitzGerald, D.M., 1993. Origin and stability of tidal inlets in Massachusetts. In: Aubrey, D.G., and Giese, G.S. (eds) Formation and Evolution of Multiple Tidal Inlets, Washington DC: AGU Coastal and Estuarine Studies, 44, pp. 1-61.

Hein, C.J., FitzGerald, D.M., Carruthers, E.A., Stone, B.D., Barnhardt, W.A., and Gontz, A.M., 2012. Refining the model of barrier island formation along a paraglacial coast in the Gulf of Maine. Marine Geology, 307-310, 40-57.

Hein, C.J., FitzGerald, D.M., Barnhardt, W.A., and Stone, B.D., 2015. Onshore-Offshore Surficial Geologic Map of the Newburyport East and Northern Half of the Ipswich Quadrangles, Massachusetts, Amherst, MA: Mass. Geological Survey, Map GM 13-01, map scale 1:24,000, 3 sheets.

Moslow, T.F., and Tye, R.S., 1985. Recognition and characterization of Holocene tidal inlet sequences. Marine Geology, 63(1), 129-151.
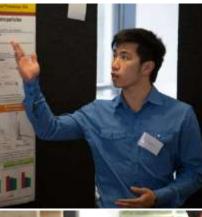
9. Acknowledgements

Presenting a Poster

- Designated time slot
  - 15-min informal talk in front of the poster
  - One-day or half-day show time
- Dress properly (more important in poster presentations)
- Printing: glossy paper, cloth, polymer
- Greet people and initiate conversations
- Control your pace and adapt to different audience
- Confidence, eye contact, do not be shy
- Extras: handouts, printouts, demos, other presenting aids
- Still need practice: a long and a short version

A good poster presentation is like a good bowl of noodles:
- Visually pleasing
- Variety
- Flexibility
- Complexity